

**Electronic Supplementary Information for:**

**Effect of Methylation in Ionic Liquids on the Gas Separation Performance of Ionic  
Liquid/Metal-Organic Framework Composites**

Vahid Nozari,<sup>a,b</sup> Muhammad Zeeshan,<sup>a,b</sup> Seda Keskin,<sup>a,b,\*</sup> and Alper Uzun<sup>a,b,\*</sup>

<sup>a</sup>Department of Chemical and Biological Engineering, Koç University, Rumelifeneri Yolu, 34450  
Sariyer, Istanbul, Turkey;

<sup>b</sup>Koç University TÜPRAŞ Energy Center (KUTEM), Koç University, Rumelifeneri Yolu, 34450  
Sariyer, Istanbul, Turkey;

\*Corresponding Authors: skeskin@ku.edu.tr and auzun@ku.edu.tr

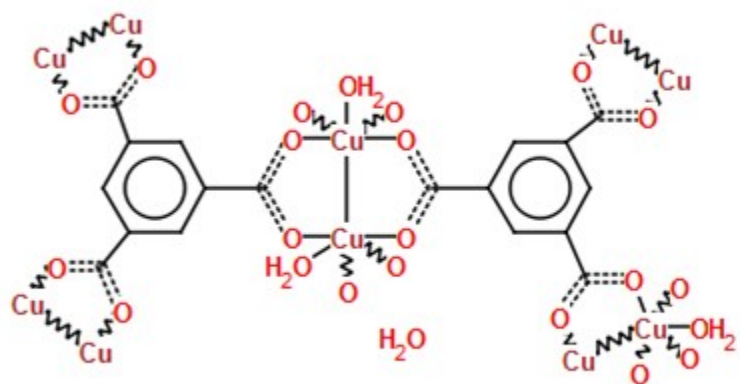


**Fig. S1.** Secondary building unit (SBU) of CuBTC.

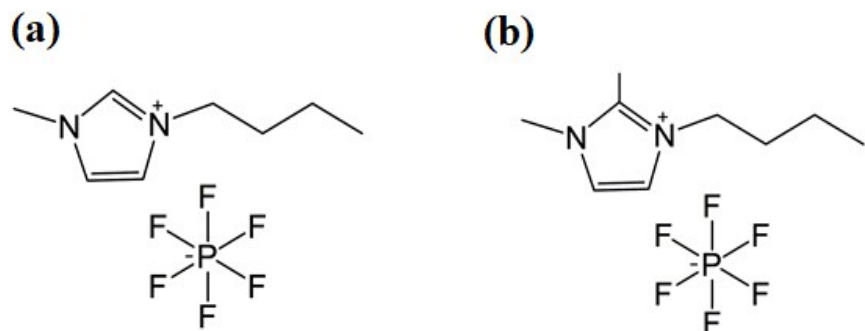


**Fig. S2.** Molecular structure of (a) [BMIM] $[\text{PF}_6]$ /CuBTC and (b) [BMMIM] $[\text{PF}_6]$ /CuBTC ILs considered in this work.

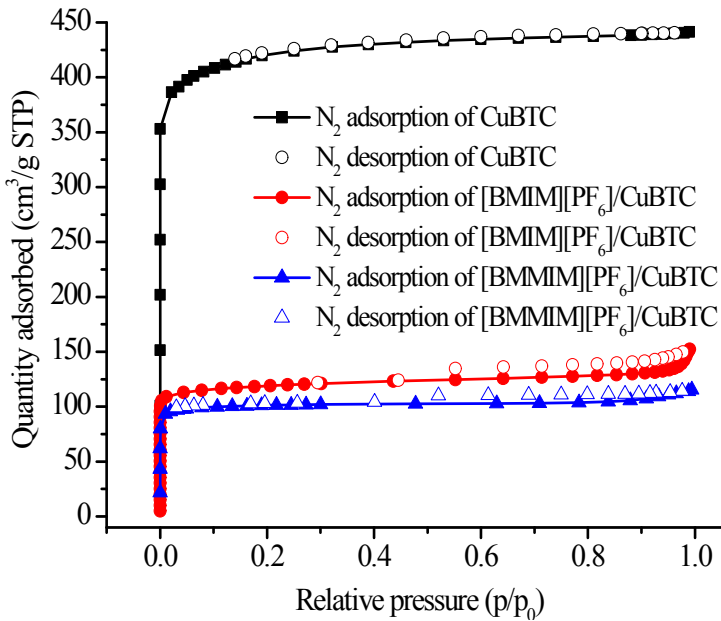


**Fig. S3.** N<sub>2</sub> adsorption isotherms of pristine CuBTC, [BMIM][PF<sub>6</sub>]/CuBTC and [BMMIM][PF<sub>6</sub>]/CuBTC samples at 77 K.

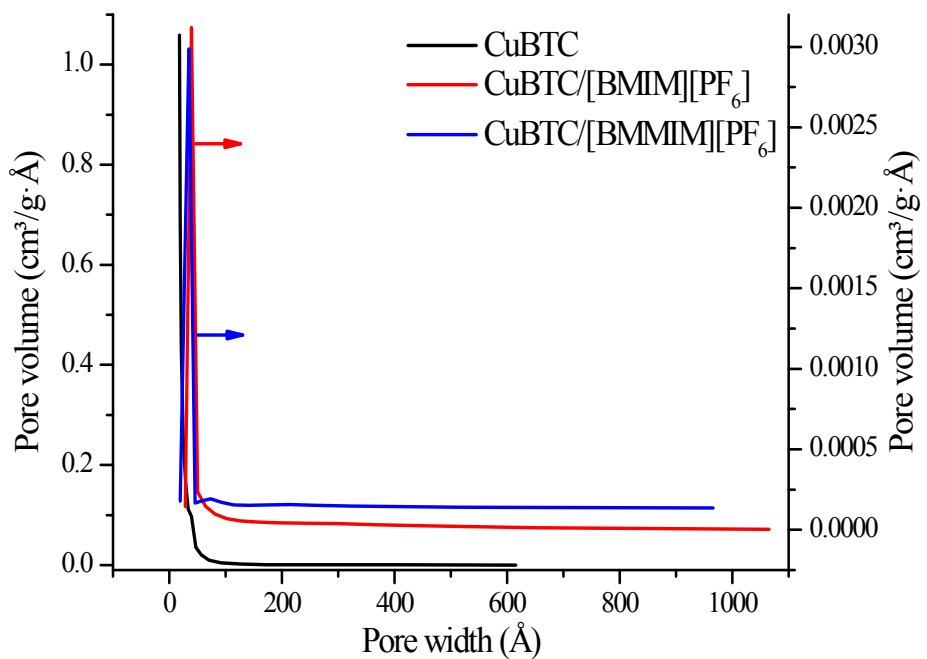


**Fig. S4.** Pore size distribution of CuBTC, [BMIM][PF<sub>6</sub>]/CuBTC and [BMMIM][PF<sub>6</sub>]/CuBTC samples obtained using the Barrett-Joyner-Halenda (BJH) method.

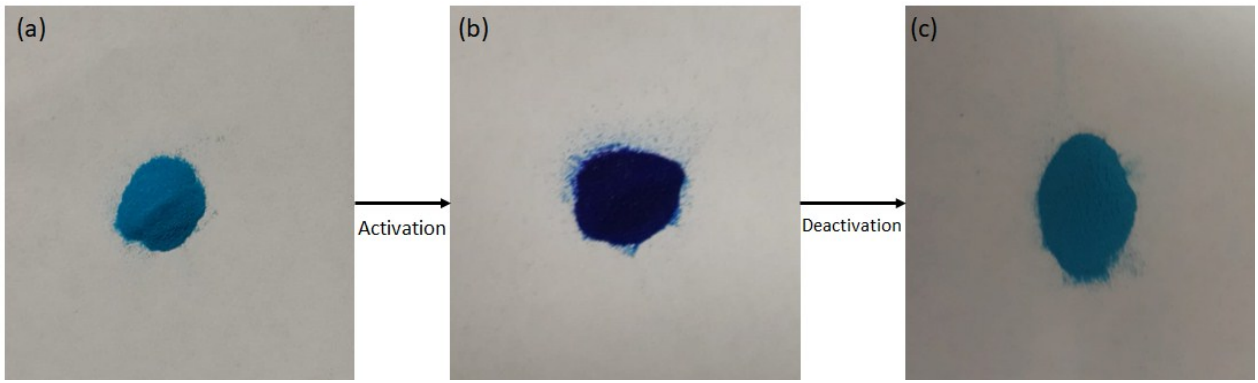


**Fig. S5.** The color change of (a) as-received CuBTC, (b) after activation under vacuum at  $10^{-3}$  bar and 105 °C for 12 hours, (c) after keeping the overnight activated sample in open atmosphere for several hours. The color changed from light to dark blue because of the removal of the moisture content, then from dark to light blue because of the atmospheric water binding onto the copper coordination sites.<sup>1</sup>

Acetone (Sigma-Aldrich, ACS reagent) was used in our sample preparation. We performed Karl Fischer titration and found that the water content was less than 5000 ppm. We also performed the IR spectroscopy characterization of the resultant sample together with that of the degassed [BMMIM][PF<sub>6</sub>]/CuBTC and [BMMIM][PF<sub>6</sub>]/CuBTC samples. The IR of the IL incorporated CuBTC samples as prepared and after degassing under vacuum at 125 °C overnight was shown in Fig. S7. IR spectrum of the freshly synthesized composite shows the presence of water molecules in the samples as expected because the sample synthesis was carried out in open air. However, IR spectra of the freshly degassed samples do not have any water features. Here, it can be inferred that the degassing of the samples under vacuum at 105 °C overnight was sufficient to remove any coordinated water and activate the samples.

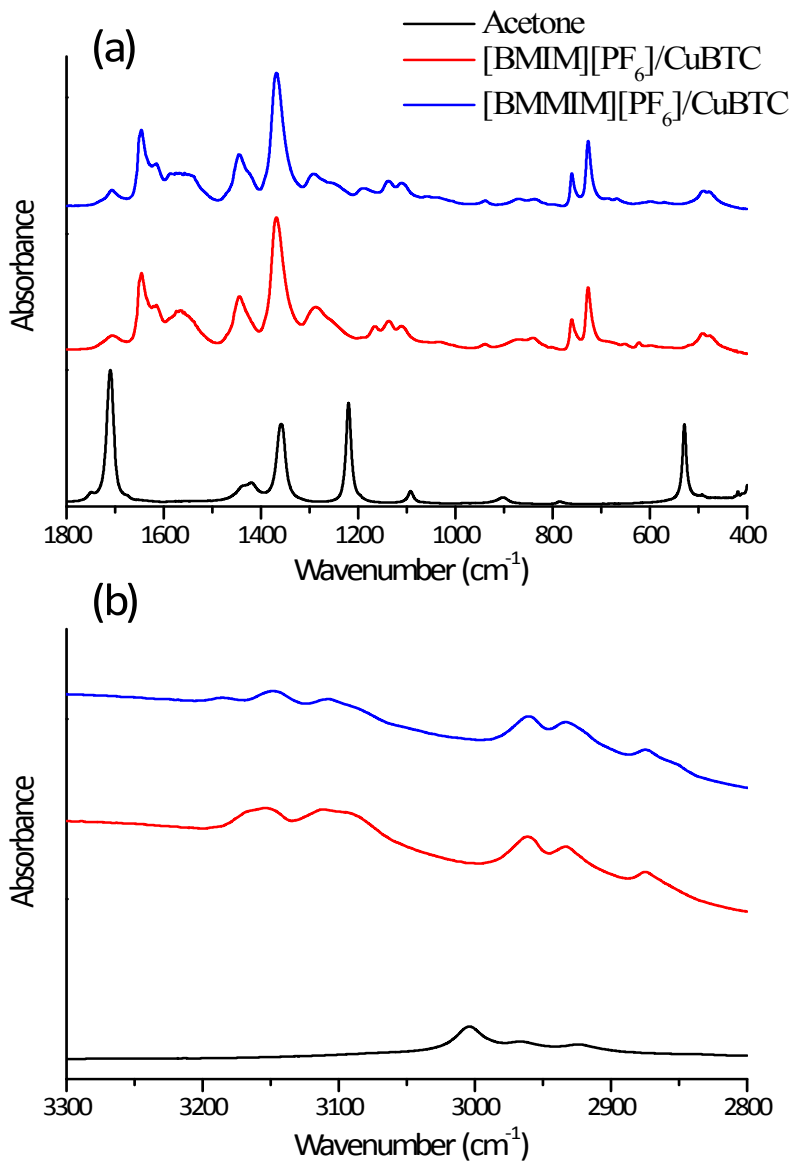


**Fig. S6.** FTIR spectra of [BMIM][PF<sub>6</sub>]/CuBTC, and [BMMIM][PF<sub>6</sub>]/CuBTC samples after drying in vacuum at 105 °C overnight; (a) 1800 and 400 ;(b) 3300 and 2800 cm<sup>-1</sup>.

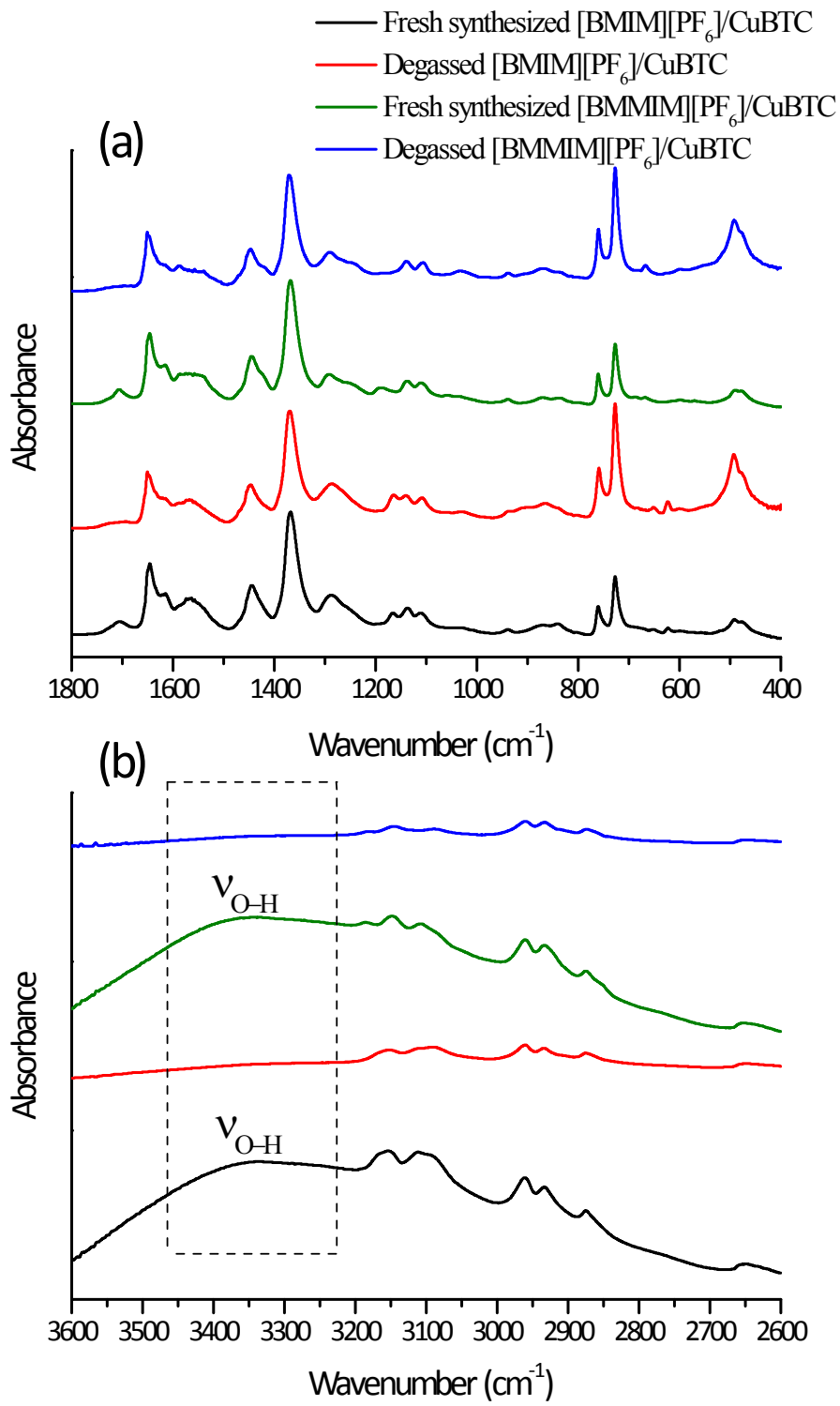


**Fig. S7.** FTIR spectra of [BMIM][PF<sub>6</sub>]/CuBTC, and [BMMIM][PF<sub>6</sub>]/CuBTC as prepared and degassed overnight samples ; (a) 1800 and 400 ;(b) 3600 and 2800 cm<sup>-1</sup>.

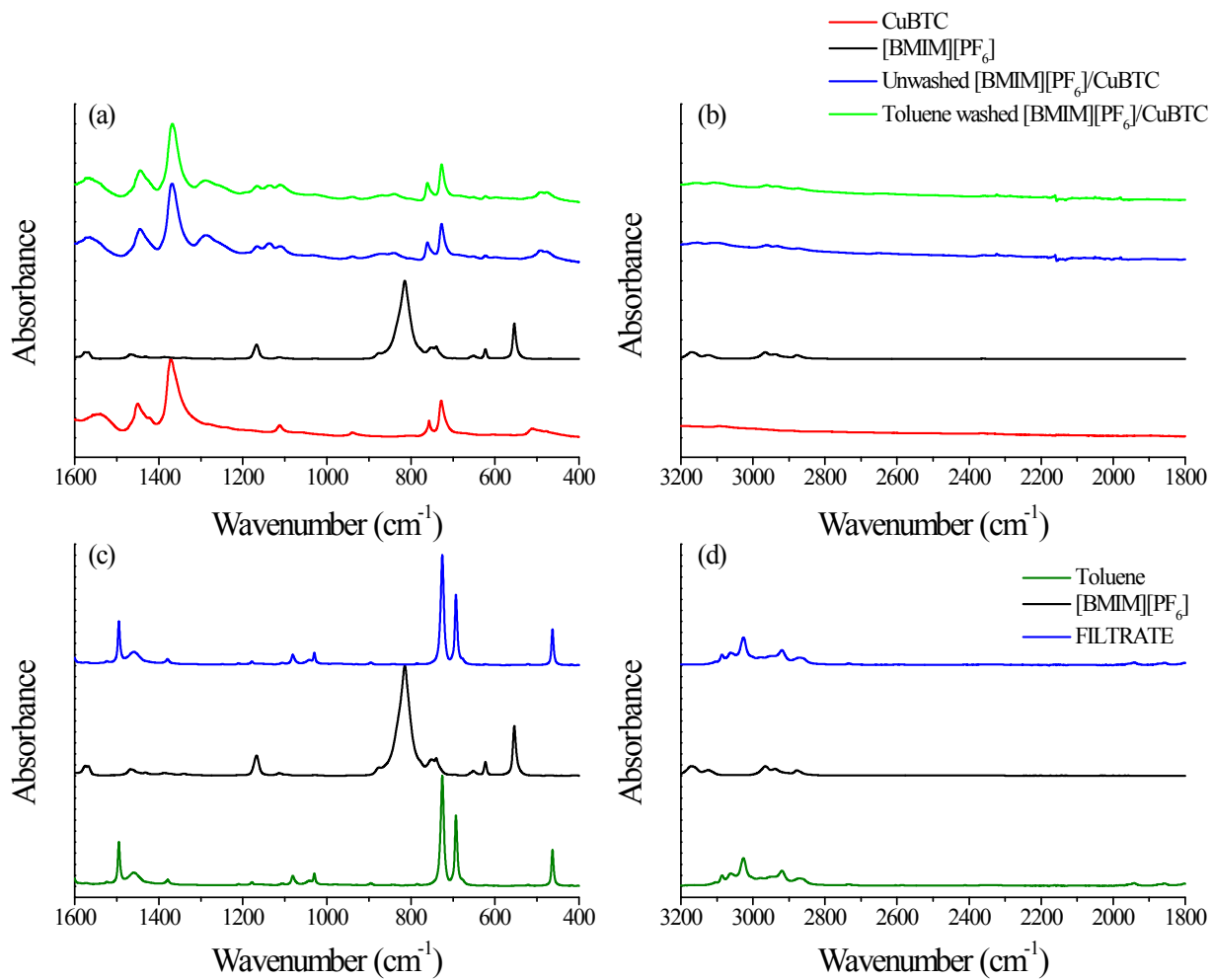


**Fig. S8.** FTIR spectra of CuBTC, bulk [BMIM][PF<sub>6</sub>], and [BMIM][PF<sub>6</sub>]/CuBTC prior and after washing with toluene in two different regions, 400-1600 cm<sup>-1</sup> and 1800-3200 cm<sup>-1</sup>; (a) and (b) Powder samples before and after washing with toluene; (c) and (d) the filtrate (liquid samples).

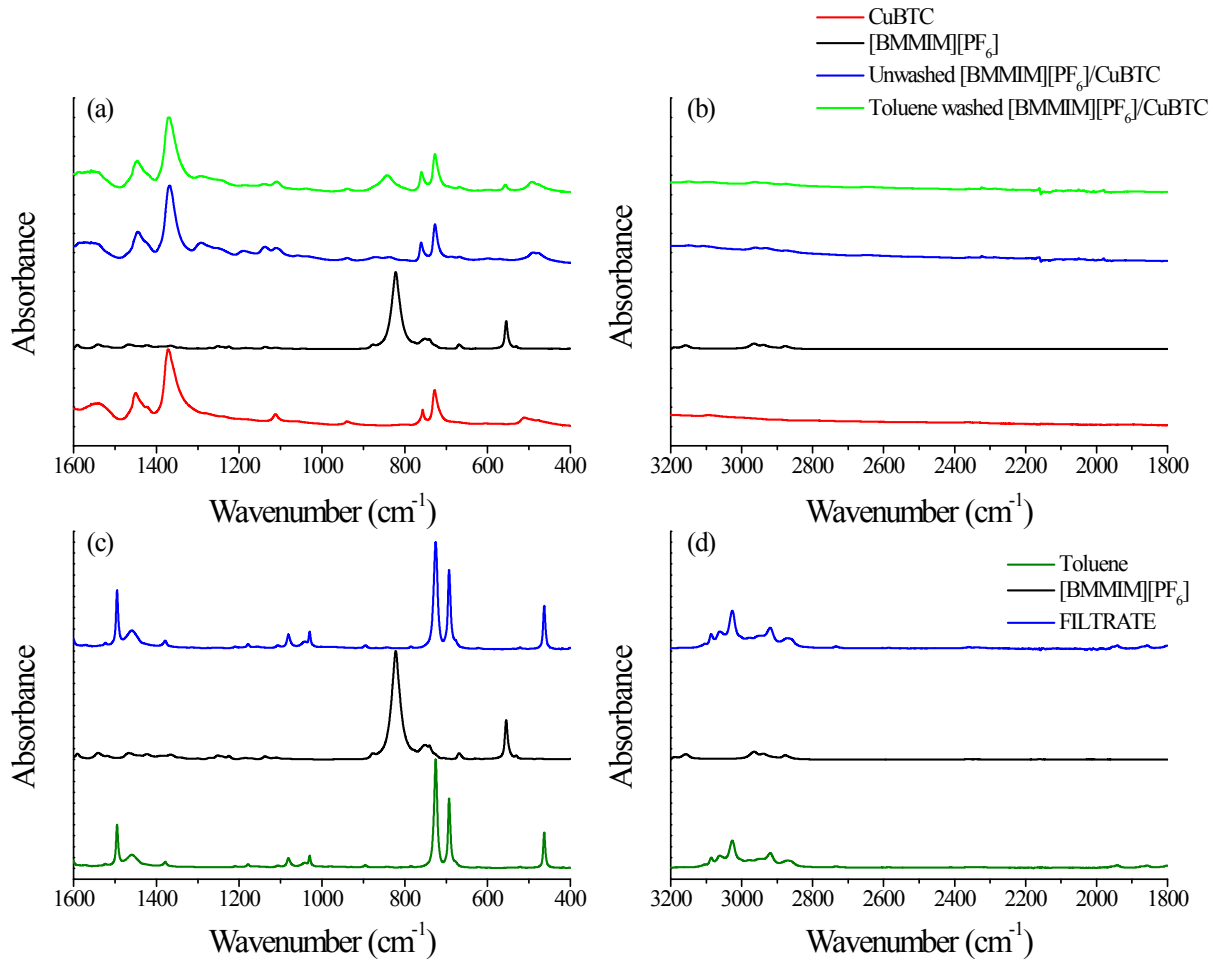


**Fig. S9.** FTIR spectra of CuBTC, bulk [BMMIM][PF<sub>6</sub>], and [BMMIM][PF<sub>6</sub>]/CuBTC prior and after washing with toluene in two different regions, 400-1600 cm<sup>-1</sup> and 1800-3200 cm<sup>-1</sup>; (a) and (b) Powder samples before and after washing with toluene; (c) and (d) the filtrate (liquid samples).

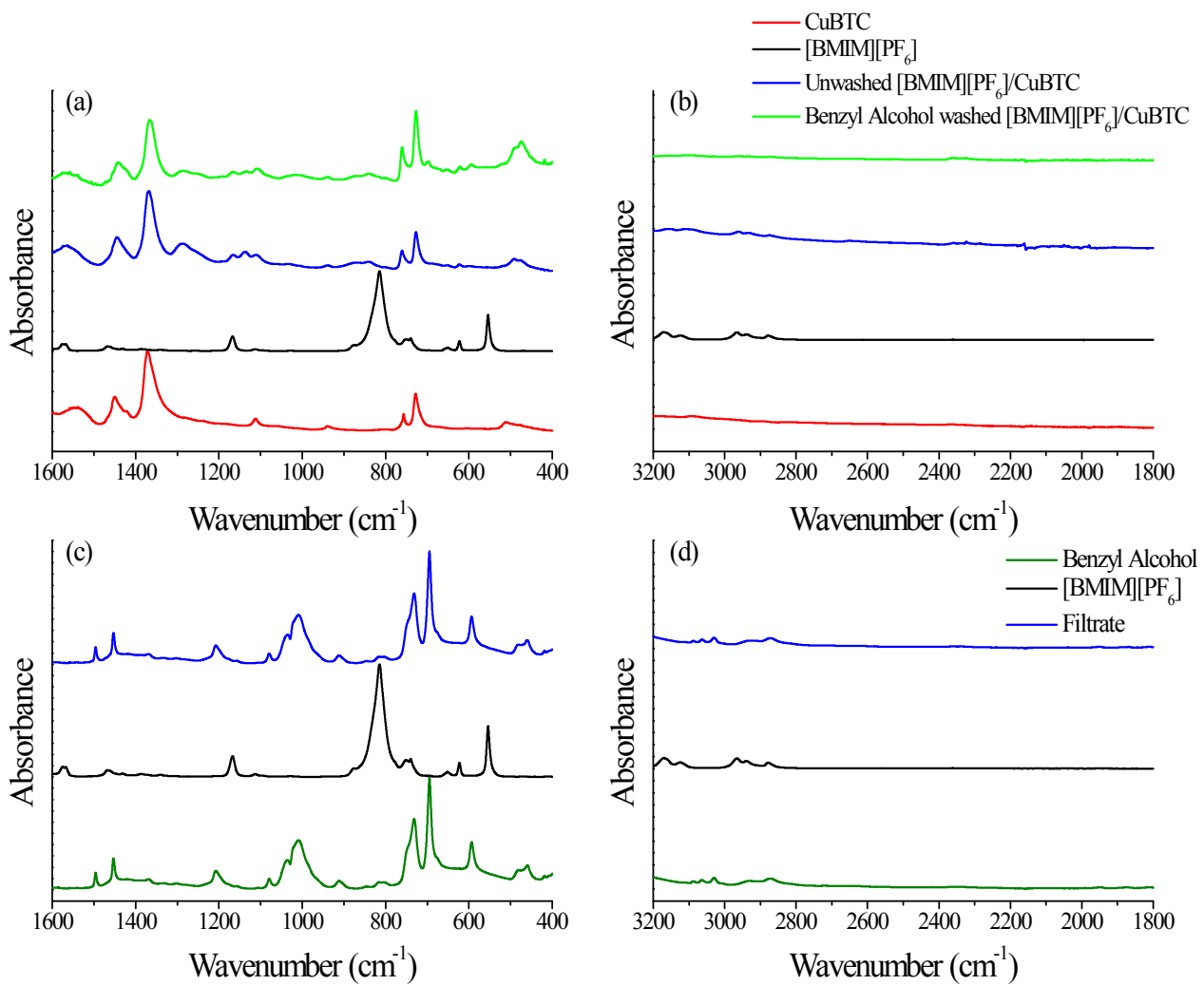


**Fig. S10.** FTIR spectra of CuBTC, bulk [BMIM][PF<sub>6</sub>], and [BMIM][PF<sub>6</sub>]/CuBTC prior and after washing with benzyl alcohol in two different regions, 400-1600 cm<sup>-1</sup> and 1800-3200 cm<sup>-1</sup>; Powder samples before and after washing with benzyl alcohol in (a) and (b); the filtrate (liquid samples) in (c) and (d).

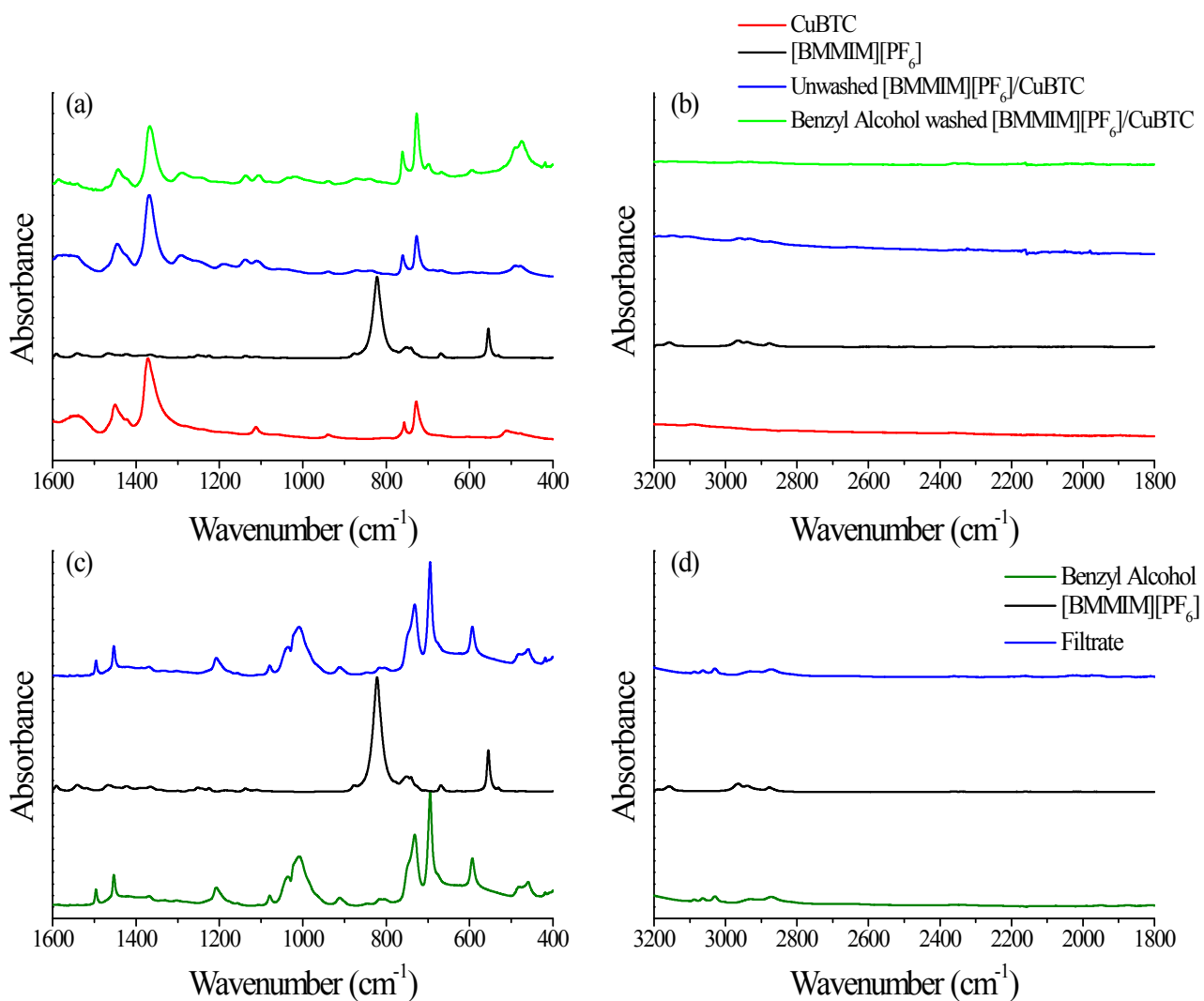


**Fig. S11.** FTIR spectra of CuBTC, bulk [BMMIM][PF<sub>6</sub>] and [BMMIM][PF<sub>6</sub>]/CuBTC prior and after washing with benzyl alcohol in two different regions, 400-1600 cm<sup>-1</sup> and 1800-3200 cm<sup>-1</sup>; Powder samples before and after washing with benzyl alcohol in (a) and (b); the filtrate (liquid samples) in (c) and (d).

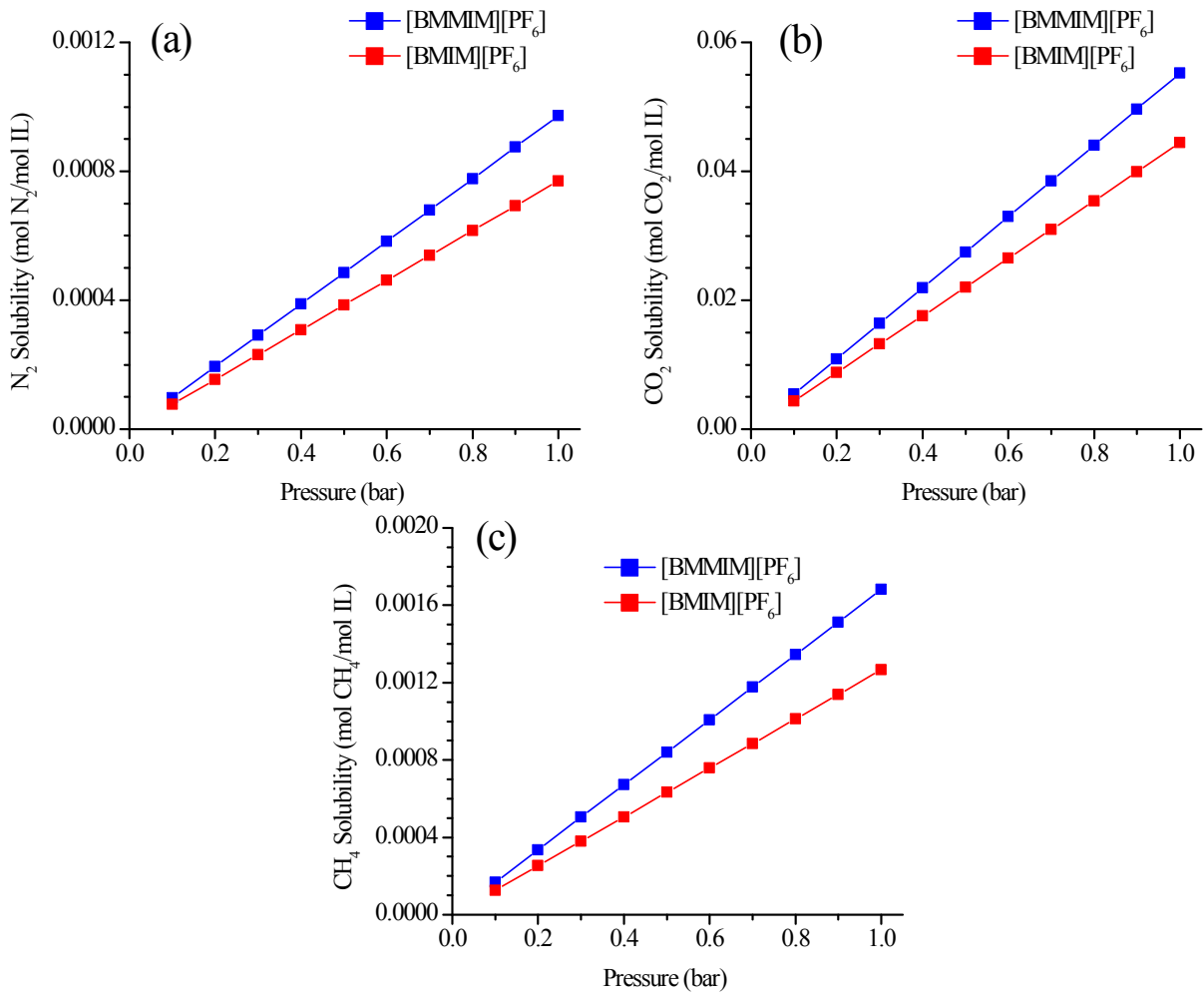


**Fig. S12.** Solubility of (a)  $N_2$ , (b)  $CO_2$ , and (c)  $CH_4$  in  $[BMIM][PF_6]$  and  $[BMMIM][PF_6]$  estimated by COSMO-RS calculations at room temperature.

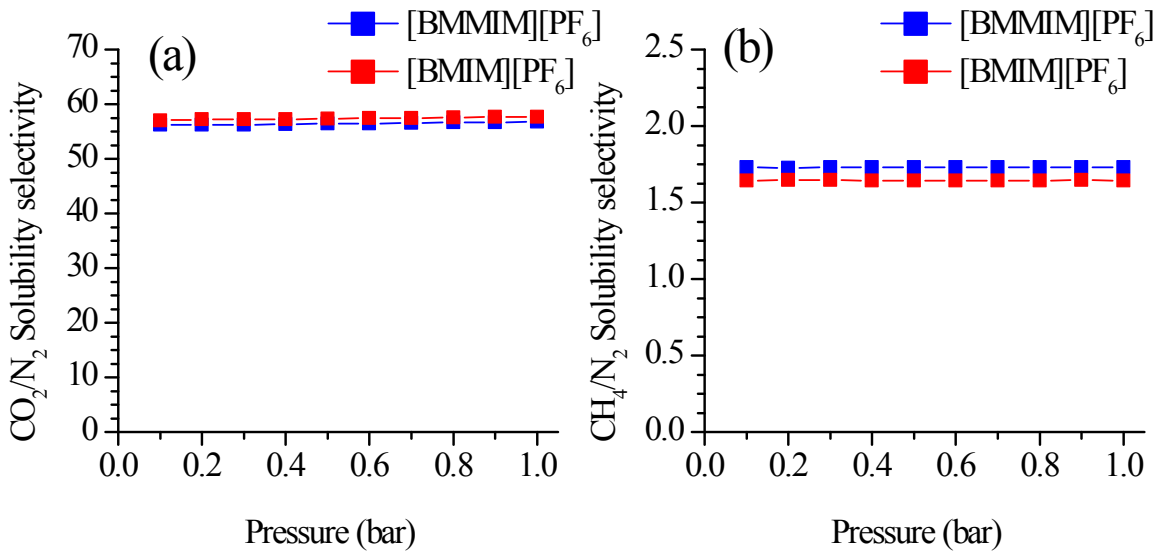


**Fig. S13.** Solubility selectivity for [BMIM][PF<sub>6</sub>] and [BMMIM][PF<sub>6</sub>] at room temperature for (a) CO<sub>2</sub>/N<sub>2</sub> and (b) CH<sub>4</sub>/N<sub>2</sub>.

**Table S1.** The Cu and P amounts in each of the IL/CuBTC samples as determined by the XRF measurements.

	[BMIM][PF <sub>6</sub> ]/CuBTC	[BMMIM][PF <sub>6</sub> ]/CuBTC
Element	Concentration (wt%)	Concentration (wt%)
CHO	76.4	80.3
Cu	21.43	17.81
P	1.67	1.67

**Table S2.** Fitted parameters using the dual-site Langmuir model for CuBTC.

CO <sub>2</sub>	$q_1$ (cc/g)	$k_1$ (1/mbar)	$q_2$ (cc/g)	$k_2$ (1/mbar)	$R^2$
	331.7031	0.2173	323.2061	0.2173	0.9999
CH <sub>4</sub>	$q_1$ (cc/g)	$k_1$ (1/mbar)	$q_2$ (cc/g)	$k_2$ (1/mbar)	$R^2$
	9.5666	1.0408	1296.35	0.01262	0.9999
N <sub>2</sub>	$q_1$ (cc/g)	$k_1$ (1/mbar)	$q_2$ (cc/g)	$k_2$ (1/mbar)	$R^2$
	535.222	0.008282	62.4115	0.04963	0.9999

**Table S3.** Fitted parameters using the dual-site Langmuir model for [BMIM][PF<sub>6</sub>]/CuBTC.

$\text{CO}_2$	$q_1$ (cc/g)	$k_1$ (1/mbar)	$q_2$ (cc/g)	$k_2$ (1/mbar)	$R^2$
	177.132	0.28352	14.7991	4.5465	0.9999
$\text{CH}_4$	$q_1$ (cc/g)	$k_1$ (1/mbar)	$q_2$ (cc/g)	$k_2$ (1/mbar)	$R^2$
	213.168	0.02983	16.9663	0.99289	0.9999
$\text{N}_2$	$q_1$ (cc/g)	$k_1$ (1/mbar)	$q_2$ (cc/g)	$k_2$ (1/mbar)	$R^2$
	0.004711	3.258*10 <sup>-13</sup>	56.314	0.07911	0.9999

**Table S4.** Fitted parameters using the dual-site Langmuir model for [BMMIM][PF<sub>6</sub>]/CuBTC.

$\text{CO}_2$	$q_1$ (cc/g)	$k_1$ (1/mbar)	$q_2$ (cc/g)	$k_2$ (1/mbar)	$R^2$
	22.4488	4.2819	95.8067	0.4385	0.9999
$\text{CH}_4$	$q_1$ (cc/g)	$k_1$ (1/mbar)	$q_2$ (cc/g)	$k_2$ (1/mbar)	$R^2$
	14.8707	1.3434	529.807	0.01526	0.9998
$\text{N}_2$	$q_1$ (cc/g)	$k_1$ (1/mbar)	$q_2$ (cc/g)	$k_2$ (1/mbar)	$R^2$
	0.53238	4.5517	272.551	0.014703	0.9999

## References

- 1 N. Al-Janabi, P. Hill, L. Torrente-Murciano, A. Garforth, P. Gorgojo, F. Siperstein and X. Fan, Mapping the Cu-BTC metal–organic framework (HKUST-1) stability envelope in the presence of water vapour for CO<sub>2</sub> adsorption from flue gases, 2015, vol. 281.